Figure S1. D2-HG-producing IDH mutation and RNA methylation
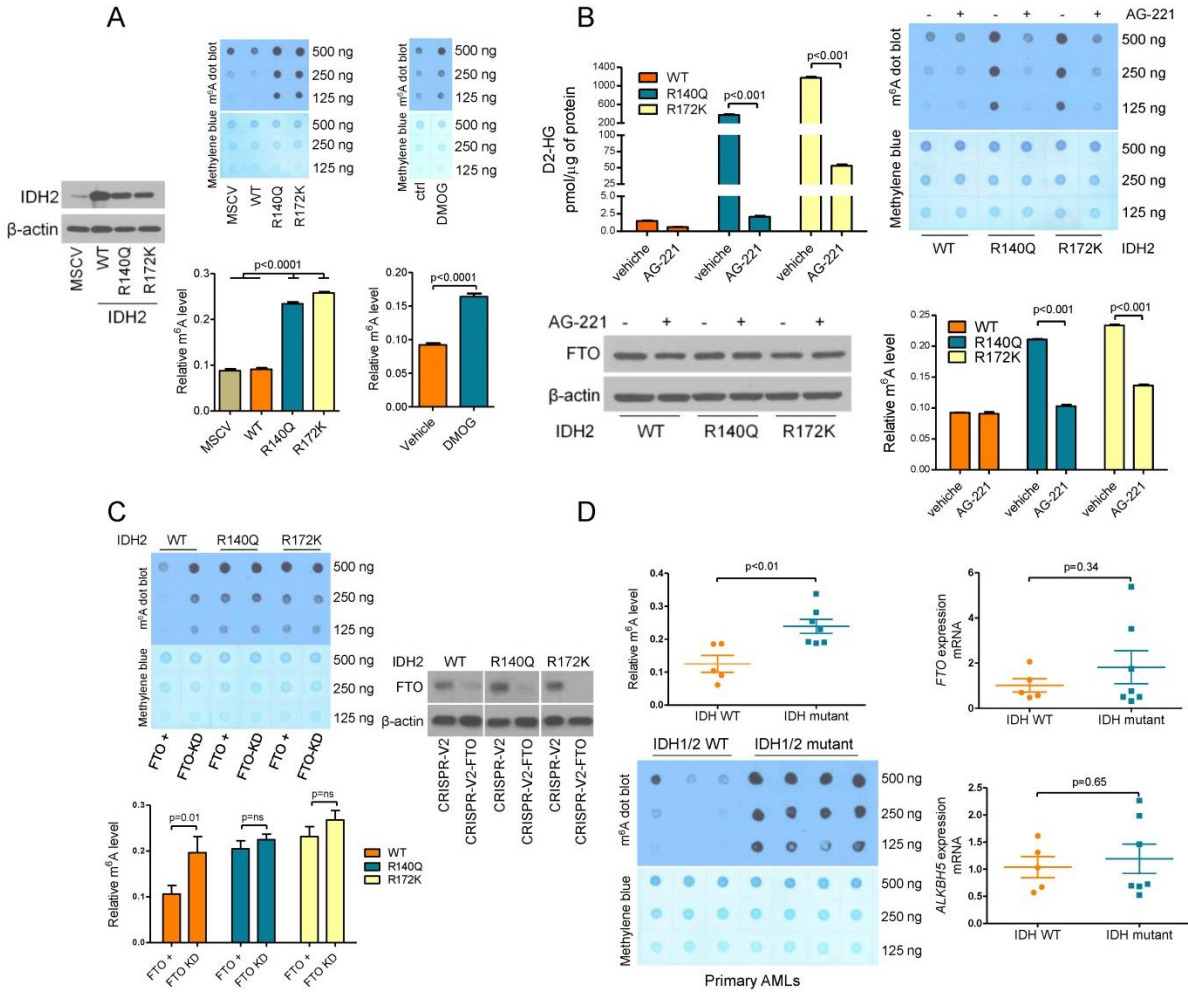
(A) Immunoblot analysis of the IDH2 protein in cells without (MSCV) or with ectopic expression of WT or mutant IDH2 as indicated (Left panel). Dot-blot and ELISA-based assay for the m^{6}A levels of cells shown in the left (Middle panels, ANOVA), and from control cells or cells treated with the α-KG competitive inhibitor DMOG (1.5 mM for 6 hr, Right panels, Student's t-test). (B) Liquid chromatography/mass spectrometry-based quantification of D-2-HG levels in cells ectopically expressing WT or mutant IDH2 that were exposed to vehicle control (DMSO) or the IDH2-mutant inhibitor AG-221 (5 µM for 24 hr) (Left top panel, Student's t-test). Immunoblot analysis of the FTO protein in lysates from these cells is shown in the bottom left panel, and dot-blot and ELISA-based assays for m^{6}A quantification are shown in the right panels (Student's t-test). (C) Dot-blot and ELISA-based assay for measurement of m^{6}A levels in cells ectopically expressing WT or mutant IDH2, with or without genetic depletion of FTO (Left panels, Student's t-test). Immunoblot analysis of the FTO protein in these same cells is shown in the panel at the right. (D) ELISA-based assay and dot-blot for quantification of m^{6}A levels in IDH1/2-mutant or WT primary AMLs (Left panels, Student's t-test). Q-RT-PCR-based quantification of *FTO* and *ALKBH5* expression in primary AMLs (Right panels, top and bottom, respectively; Student's t-test). All error bars depict +/- SD.

Supplemental Experimental Procedures:

IDH2 genetic models: The wild-type IDH2 coding sequence was PCR amplified and cloned into the MSCV-eGFP retrovirus system. Site direct mutagenesis was used to create the R140Q and R172K variants in the same plasmid background. All constructs were sequenced verified. Retrovirus generation and HEK-293T cell transduction were performed as we described. Efficiency of transduction was determined by FACS analysis, and cell sorting performed if percentage of GFP positive cells was below 80%. Cell lines were validated by STR profiling and tested for Mycoplasma contamination by PCR.

FTO KO models: Two unique guideRNA sequences directed at exon 1 (g1) and exon 3 (g2) of the human FTO gene were independently cloned into the lentivirus vector CRISPR-V2-puromycin (Addgene plasmid # 52961; (Sanjana et al., 2014). Viruses were co-transduced into HEK-293T cells stably expressing IDH2-WT, IDH2-R140Q or IDH2-R172K and cells selected with puromycin (0.5µg/ml to 1.0 µg/ml). Efficiency of the FTO KO in the polyclonal populations was determined by western blotting; Targeting sequences, g1: 5'GACTGCCGAGGAACGAGAGC3' (exon 1); g2: 5'GTATCTCGCATCCTCATTGG 3' (exon 3). IDH2-WT, IDH2-R140Q or IDH2-R172K control cells were generated with transduction of "empty" CRISPR-V2 lentivirus, followed by puromycin selection.

RNA methylation assays: m^6A levels were quantified with two methodologies: 1) An ELISA-based EpiQuik™ m6A RNA Methylation Quantification Kit (Epigentek # P-9005), used according to the manufacturer guidelines. In this assay, abundance of m^6A marks was quantified by absorbance and reported as relative values to the negative and positive controls, an RNA containing no m^6A and an m^6A oligo normalized to have 100% of m^6A. All assays were performed in triplicate and biological replicates were completed at least 3 times. For cell line models and primary AMLs, we utilized 200ng and 100ng of total RNA per well, respectively. Cell line data shown are mean ± SD of an assay performed in triplicate or the combination of three independent biological replicates (Figure S1C); all assays were confirmed in at least three biological replicates. 2) An m^6A dot-blot assay implemented with an anti-m^6A antibody (clone 212B11, Synaptic Systems) and performed exactly as by Li et al., except for one minor change - the RNAs were loaded directly on the membrane followed by UV cross-link, without the use of the Bio-Dot apparatus. The dot-blot assay was performed for all cell line models examined and for a subset of primary AMLs with sufficient RNA available. In all applications, RNA was isolated using the Trizol method and quantified by UV spectrophotometry.

Metabolite extraction and quantification by liquid chromatography mass spectrometry (LC/MS): HEK-293T cells stably expressing IDH2 WT, IDH2 R140Q or IDH2R172K, exposed for 24 hr to 5 µM of AG-221 or vehicle control, were gently washed in PBS, collected and flash-frozen in dry ice. The metabolites extraction and processing of the samples for D2-HG analysis was as performed as we described in details earlier (Lin et al). In brief, HPLC-ESI-MS (high performance liquid chromatography-electrospray ionization-mass spectrometry) analyses were conducted on a Thermo Fisher Q Exactive mass spectrometer with online separation by a Thermo Fisher/Dionex Ultimate 3000 HPLC. The conditions used to separate D-2-HG from L-2-HG analyses were: column, Kinetex C18, 2.6 µm, 2.1 x 100mm (Phenomenex); mobile phase, 1% acetonitrile with 125 mg l⁻1 ammonium formate, pH 3.6; flow rate, 400 µl min⁻1. For all analyses, full scan mass spectra were acquired in the orbitrap using negative ion detection over a range of *m/z* 100–800 at 70,000 resolution (*m/z* 300). Metabolite identification was based on the metabolite accurate mass (±5 p.p.m.) and in agreement with the HPLC retention time of authentic standards. Quantification was made by integration of extracted ion chromatograms of each metabolite followed by comparison with the corresponding standard curves.

Compounds: Relevant cell line models were exposed to 1.5 mM of dimethyloxalylglycine (DMOG; Frontier Scientific) for 6 hr, or to 5 µM of AG-221 (Enasidenib, ChemieTek) for 24 hr.

Western blotting: Whole-cell lysates were extracted from relevant cell models, quantified, separated by sodium dodecyl sulfate-polyacrylamide gel electrophoresis (SDS-PAGE), and transferred to polyvinylidene difluoride membrane. Proteins were detected with specific antibodies directed at IDH2 (Abcam, #ab55271), FTO (Santa Cruz, C-3 sc#271713), β-actin (Sigma-Aldrich, #A2228).

Q-RT-PCR: Expression of *FTO* and *ALKBH5* in primary AMLs was determined by real-time RT-PCR. Following RNA isolation, cDNA was generated using the Applied Biosystems High Capacity cDNA Reverse Transcription kit. Subsequently, all amplifications were performed in triplicate using the SYBR green method in the AB StepOne Plus detection system. The expression of the target genes was normalized to that of house-keeping controls (TATA-Binding protein, TBP, and Actin), quantification implemented using the ΔΔCT method and relative expression defined as $2^{-\Delta\Delta CT}$. FTO primers, Fw: 5' AACGAGAGCGCGAAGCTAAG 3', Rv: 5' CTCCTCAGATACACTGCTGG 3'. ALKBH5 primers: Fw: 5' TTCGGCTGCAAGTTCCAGTTC 3', Rv: 5' TTGATGTCCTGAGGCCGTATG 3'

Statistics: Analyses were performed using a one-way ANOVA, with Bonferroni's multiple comparison post-hoc tests, and by two-tailed Student's t-test. Equal variance was determined with an F-test. $P<0.05$ was considered significant. Data analyses were performed in the Prism software (version 5.02, GraphPad Software Inc) and Excel (Microsoft).

Primary AMLs: Leukemia specimens were obtained from adult patients with AML, diagnosed at the Division of Hematology, Medical University of Graz, Austria. Biobanking was performed in accordance with institutional guidelines and written informed consent was obtained from each subject. Use of anonymized samples was approved by Review Boards of the Medical University of Graz, Austria, and UT Health Science Center at San Antonio, USA. In addition to cytogenetics, molecular analysis of a panel of 19 or 39 genes implicated in hematological cancers was performed by targeted deep sequencing, as described (Lal et al., 2017). For AMLs #8242 to #8686 the genes sequenced were: *CEBPA*; *DNMT3A*; GATA2; *TP53* (entire coding sequence); *TET2* (exon 3-11); *NPM1* (exon 11); *FLT3* (exons 14-16, 20, 21); *ASXL1* (exon 12); *CBL* (exons 8, 9); *IDH1* (exon 4); *IDH2* (exon 4); *JAK2* (exon 13); *KIT* (exons 8, 10, 11, 17); *KRAS* (exon 2, 3); *NRAS* (exon 2, 3); *PTPN11* (exon 3, 13); *RUNX1* (exons 3-8); *WT1* (exon 7, 9); *BRAF* (hotspot exon 15). For samples number #8766 to #8946, an additional 20 genes were examined, including: *BCOR*; *DDX41*; *ETV6*; *NF1*; *PHF6*; *SF3B2*; *SFRP1*; *SRP72*; *STAG2*; *ZRSR2* (entire coding sequence); *CALR* (exon 9); *CSF3R* (exons 14-17); *ETNK1* (exon 3); *EZH2* (exons 16-19); *MPL* (exon 10); *SETBP1* (hotspot exon 4); *SF3B1* (exon 14-16); *SRSF2* (hotspot exon 1); *STAT3* (exons 20, 21); *U2AF1* (exon 2, 7, 9). All analyses were performed in duplicates.

Clinical, cytogenetic and molecular characteristics of primary AML specimens analyzed in this study are listed below.

ID	Age	Sex	Type	Cytogenetics	IDH1/2 status	other mutations	Source/%blast
8242	69	M	de novo	n.d.	IDH2 R140Q	-	PB/63%
8259	65	F	de novo	46,XX[20]	IDH1 R132C	NRAS, PTPN11	BM/90%
8438	88	F	de novo	45~47,XX,+11[cp19]/46,XX[1]	IDH2 R140Q	-	PB/80%
8444	54	M	tAML	47,XY,+8[5]/46,XY[15]	IDH2 R172K	RUNX1, CEBPA	BM/70%
8488	71	F	de novo	46,XX	IHD2 R140Q	NPM1, FLT3 ITD, DNMT3A	PB/90%
8686	58	F	de novo	45~46,XX,?t(6;11)(q27;q23)[cp7]	IDH2 R140Q	NRAS, KRAS	BM/80%
8766	67	F	de novo - relapse	46,XX	WT	NPM1	PB/70%
8777	54	F	de novo	46,XX[19]	WT	DNMT3A, TET2, PTPN11, RUNX1	BM/60%
8824	46	F	de novo	46,XX[19]	WT	FLT3	PB/70%
8913	76	M	de novo	46,XY[15]	WT	NPM1, TET2, MAF	PB/90%
8931	84	M	tAML	42~44,XY,t(1;2)(p34;p32)[4], der(5)t(5;13)(q11.2;q22)[16], dic(12;16)(p11.2;p11.2)[16],-13[16],-16[16]/46,XY[2]	WT	TET2, TP53	BM/60%
8946	48	M	de novo -relapse	47,XY,+4	IDH1 R132H	DNMT3A, NPM1, KIT	PB/70%

PB = peripheral blood; BM = bone marrow

Supplemental References:

Lal, R., Lind, K., Heitzer, E., Ulz, P., Aubell, K., Kashofer, K., Middeke, J. M., Thiede, C., Schulz, E., Rosenberger, A., *et al.* (2017). Somatic TP53 mutations characterize preleukemic stem cells in acute myeloid leukemia. Blood. doi 10.1182/blood-2016-11-751008

Sanjana, N. E., Shalem, O., and Zhang, F. (2014). Improved vectors and genome-wide libraries for CRISPR screening. Nature methods *11*, 783-784.